This article was downloaded by: [University of California, San Diego]
On: 22 August 2012, At: 09:07
Publisher: Taylor & Francis
Informa Ltd Registered in England and Wales Registered Number: 1072954
Registered office: Mortimer House, 37-41 Mortimer Street, London W1T 3JH, UK

Molecular Crystals and Liquid Crystals

Publication details, including instructions for authors and subscription information:
http://www.tandfonline.com/loi/gmcl20

Structure of Chiral Isotropic Phases

W. Józefowicz [a], M. Cieśla [a] & L. Longa [a b]

[a] Marian Smoluchowski Institute of Physics, Department of Statistical Physics and Mark Kac Complex Systems Research Center, Jagellonian University, Reymonta, Kraków, Poland

[b] Liquid Crystal Institute, Kent State University, Kent, USA

Version of record first published: 31 Aug 2006

To cite this article: W. Józefowicz, M. Cieśla & L. Longa (2005): Structure of Chiral Isotropic Phases, Molecular Crystals and Liquid Crystals, 438:1, 9/[1573]-16/[1580]

To link to this article: http://dx.doi.org/10.1080/15421400590954948

PLEASE SCROLL DOWN FOR ARTICLE

Full terms and conditions of use: http://www.tandfonline.com/page/terms-and-conditions

This article may be used for research, teaching, and private study purposes. Any substantial or systematic reproduction, redistribution, reselling, loan, sub-licensing, systematic supply, or distribution in any form to anyone is expressly forbidden.

The publisher does not give any warranty express or implied or make any representation that the contents will be complete or accurate or up to date. The accuracy of any instructions, formulae, and drug doses should be independently verified with primary sources. The publisher shall not be liable

for any loss, actions, claims, proceedings, demand, or costs or damages whatsoever or howsoever caused arising directly or indirectly in connection with or arising out of the use of this material.

Downloaded by [University of California, San Diego] at 09:07 22 August 2012

Mol. Cryst. Liq. Cryst., Vol. 438, pp. 9/[1573]–16/[1580], 2005
Copyright © Taylor & Francis Inc.
ISSN: 1542-1406 print/1563-5287 online
DOI: 10.1080/15421400590954948

Taylor & Francis
Taylor & Francis Group

Downloaded by [University of California, San Diego] at 09:07 22 August 2012

Structure of Chiral Isotropic Phases

W. Józefowicz
M. Cieśla
Marian Smoluchowski Institute of Physics, Department of Statistical Physics and Mark Kac Complex Systems Research Center, Jagellonian University, Reymonta, Kraków, Poland

L. Longa
Marian Smoluchowski Institute of Physics, Department of Statistical Physics and Mark Kac Complex Systems Research Center, Jagellonian University, Reymonta, Kraków, Poland and Liquid Crystal Institute, Kent State University, Kent, USA

We present computer simulation studies of the model chiral liquid crystal as introduced by Memmer [1,2]. The analysis of resulting structures is based on the two-point correlation modes [3] and on calculations of the excess specific heat. Our aim is to characterize the isotropic phases and to search for a critical point between the isotropic liquid and BPIII.

Keywords: chiral liquid; correlations; MC simulation

I. INTRODUCTION

Correlation profiles are essential for a proper understanding of thermodynamic behavior of chiral liquid crystals. For example, recent theoretical studies prove that the phase diagram involving the blue phases is fundamentally governed by the pair correlations between orientational degrees of freedom [3–5]. Also many physical properties

This work was supported by the Polish projects (KBN) Nos. 5 P03B 052 20 and 2 P03B 086 23 . We also gratefully acknowledge the computing grant G27-8 towards the use of the ICM (University of Warsaw) computers.

Address correspondence to W. Józefowicz, Marian Smoluchowski Institute of Physics, Department of Statistical Physics and Mark Kac Complex Systems Research Center, Jagellonian University, Reymonta 4, Kraków, Poland. E-mail: wojtek@dalidor.if.uj.edu.pl

measured in experiments, as e.g., the excess heat capacity and the optical activity [3], can be expressed as integrals involving the two-point correlation functions. We believe this indicates on an intrinsic interest in studying the correlations in the chiral liquid crystals.

In this work we report on the shape of the two-point correlation function as obtained from Monte-Carlo (MC) simulation for the model system [1,2]. The excess heat capacity data are also presented to strengthen our conclusions. The paper is organized as follows. In the next section we introduce the theoretical framework with which to analyze the two-point correlations. We also define the system used in simulations. Then some of the results are shown.

II. THEORETICAL BACKGROUND

A common approach to describe orientational properties of liquid crystals is one that refers to a traceless and symmetric tensor field $\mathbf{Q}(\boldsymbol{r})$.The tensor could be defined on a mesoscopic scale or at the molecular level using molecule-fixed tripod of vectors. Here we refer to the second possibility and assume that molecules forming a liquid crystal are uniaxial. Characterizing each molecule by the orientation of its long axis, specified by the unit vector Ω, we introduce the tensor $\mathbf{Q}(\boldsymbol{r})$ as

$$\mathbf{Q}(\boldsymbol{r}) = \Omega(\mathbf{r}) \otimes \Omega(\mathbf{r}) - \frac{1}{3}\mathbf{1}. \tag{1}$$

With the help of $\mathbf{Q}$ the two-point correlation function is given by $\langle \mathbf{Q}(\boldsymbol{r}) \otimes \boldsymbol{Q}(\mathbf{r}')\rangle$,where the average denoted as $\langle ... \rangle$ is taken over a statistical ensemble. A full mathematical analysis of this quantity is presented in our recent article [3]. Following that paper the correlation function of a chiral isotropic liquid could be divided into five uniaxial modes of angular momenta $L = 0,1, \ldots, 4$

$$\langle \mathbf{Q}(\boldsymbol{r}) \otimes \mathbf{Q}(\boldsymbol{r}')\rangle = \mathbf{G}(\boldsymbol{r} - \boldsymbol{r}') = \sum_{L=0}^{4} G^{(L)}(|\boldsymbol{r} - \boldsymbol{r}'|)\mathbf{M}_0^{(L)}\left(\frac{\boldsymbol{r} - \boldsymbol{r}'}{|\boldsymbol{r} - \boldsymbol{r}'|}\right), \tag{2}$$

where the basis tensors are given by

$$\begin{aligned}\boldsymbol{M}_0^{(0)} = \frac{1}{6\sqrt{5}}[&6(\hat{\boldsymbol{x}} \otimes \hat{\boldsymbol{x}} \otimes \hat{\boldsymbol{x}} \otimes \hat{\boldsymbol{x}} + \hat{\boldsymbol{y}} \otimes \hat{\boldsymbol{y}} \otimes \hat{\boldsymbol{y}} \otimes \hat{\boldsymbol{y}} + \hat{\boldsymbol{z}} \otimes \hat{\boldsymbol{z}} \otimes \hat{\boldsymbol{z}} \otimes \hat{\boldsymbol{z}}) \\ &- 2(\hat{\boldsymbol{x}} \otimes \hat{\boldsymbol{x}} + \hat{\boldsymbol{y}} \otimes \hat{\boldsymbol{y}} + \hat{\boldsymbol{z}} \otimes \hat{\boldsymbol{z}}) \otimes (\hat{\boldsymbol{x}} \otimes \hat{\boldsymbol{x}} + \hat{\boldsymbol{y}} \otimes \hat{\boldsymbol{y}} + \hat{\boldsymbol{z}} \otimes \hat{\boldsymbol{z}}) \\ &+ 3((\hat{\boldsymbol{x}} \otimes \hat{\boldsymbol{y}} + \hat{\boldsymbol{y}} \otimes \hat{\boldsymbol{x}}) \otimes (\hat{\boldsymbol{x}} \otimes \hat{\boldsymbol{y}} + \hat{\boldsymbol{y}} \otimes \hat{\boldsymbol{x}}) \\ &+ (\hat{\boldsymbol{x}} \otimes \hat{\boldsymbol{z}} + \hat{\boldsymbol{z}} \otimes \hat{\boldsymbol{x}}) \otimes (\hat{\boldsymbol{x}} \otimes \hat{\boldsymbol{z}} + \hat{\boldsymbol{z}} \otimes \hat{\boldsymbol{x}}) \\ &+ (\hat{\boldsymbol{y}} \otimes \hat{\boldsymbol{z}} + \hat{\boldsymbol{z}} \otimes \hat{\boldsymbol{y}}) \otimes (\hat{\boldsymbol{y}} \otimes \hat{\boldsymbol{z}} + \hat{\boldsymbol{z}} \otimes \hat{\boldsymbol{y}}))],\end{aligned} \tag{3}$$

Downloaded by [University of California, San Diego] at 09:07 22 August 2012

$$\begin{aligned}\boldsymbol{M}_0^{(1)} = \frac{-i}{2\sqrt{10}}[&2(\hat{\boldsymbol{x}}\otimes\hat{\boldsymbol{x}} - \hat{\boldsymbol{y}}\otimes\hat{\boldsymbol{y}})\otimes(\hat{\boldsymbol{x}}\otimes\hat{\boldsymbol{y}} + \hat{\boldsymbol{y}}\otimes\hat{\boldsymbol{x}})\\ &- 2(\hat{\boldsymbol{x}}\otimes\hat{\boldsymbol{y}} + \hat{\boldsymbol{y}}\otimes\hat{\boldsymbol{x}})\otimes(\hat{\boldsymbol{x}}\otimes\hat{\boldsymbol{x}} - \hat{\boldsymbol{y}}\otimes\hat{\boldsymbol{y}})\\ &+ (\hat{\boldsymbol{x}}\otimes\hat{\boldsymbol{z}} + \hat{\boldsymbol{z}}\otimes\hat{\boldsymbol{x}})\otimes(\hat{\boldsymbol{y}}\otimes\hat{\boldsymbol{z}} + \hat{\boldsymbol{z}}\otimes\hat{\boldsymbol{y}})\\ &- (\hat{\boldsymbol{y}}\otimes\hat{\boldsymbol{z}} + \hat{\boldsymbol{z}}\otimes\hat{\boldsymbol{y}})\otimes(\hat{\boldsymbol{x}}\otimes\hat{\boldsymbol{z}} + \hat{\boldsymbol{z}}\otimes\hat{\boldsymbol{x}})],\end{aligned} \tag{4}$$

$$\begin{aligned}\boldsymbol{M}_0^{(2)} = \frac{1}{6\sqrt{14}}[&4\hat{\boldsymbol{x}}\otimes\hat{\boldsymbol{x}}\otimes(\hat{\boldsymbol{x}}\otimes\hat{\boldsymbol{x}} - 2\hat{\boldsymbol{y}}\otimes\hat{\boldsymbol{y}} + \hat{\boldsymbol{z}}\otimes\hat{\boldsymbol{z}})\\ &+ 4\hat{\boldsymbol{z}}\otimes\hat{\boldsymbol{z}}\otimes(\hat{\boldsymbol{x}}\otimes\hat{\boldsymbol{x}} + \hat{\boldsymbol{y}}\otimes\hat{\boldsymbol{y}} - 2\hat{\boldsymbol{z}}\otimes\hat{\boldsymbol{z}})\\ &+ 4\hat{\boldsymbol{y}}\otimes\hat{\boldsymbol{y}}\otimes(\hat{\boldsymbol{y}}\otimes\hat{\boldsymbol{y}} - 2\hat{\boldsymbol{x}}\otimes\hat{\boldsymbol{x}} + \hat{\boldsymbol{z}}\otimes\hat{\boldsymbol{z}})\\ &+ 6(\hat{\boldsymbol{x}}\otimes\hat{\boldsymbol{y}} + \hat{\boldsymbol{y}}\otimes\hat{\boldsymbol{x}})\otimes(\hat{\boldsymbol{x}}\otimes\hat{\boldsymbol{y}} + \hat{\boldsymbol{y}}\otimes\hat{\boldsymbol{x}})\\ &- 3(\hat{\boldsymbol{x}}\otimes\hat{\boldsymbol{z}} + \hat{\boldsymbol{z}}\otimes\hat{\boldsymbol{x}})\otimes(\hat{\boldsymbol{x}}\otimes\hat{\boldsymbol{z}} + \hat{\boldsymbol{z}}\otimes\hat{\boldsymbol{x}})\\ &- 3(\hat{\boldsymbol{y}}\otimes\hat{\boldsymbol{z}} + \hat{\boldsymbol{z}}\otimes\hat{\boldsymbol{y}})\otimes(\hat{\boldsymbol{y}}\otimes\hat{\boldsymbol{z}} + \hat{\boldsymbol{z}}\otimes\hat{\boldsymbol{y}})],\end{aligned} \tag{5}$$

$$\begin{aligned}\boldsymbol{M}_0^{(3)} = \frac{-i}{2\sqrt{10}}[&(\hat{\boldsymbol{x}}\otimes\hat{\boldsymbol{x}} - \hat{\boldsymbol{y}}\otimes\hat{\boldsymbol{y}})\otimes(\hat{\boldsymbol{x}}\otimes\hat{\boldsymbol{y}} + \hat{\boldsymbol{y}}\otimes\hat{\boldsymbol{x}})\\ &- (\hat{\boldsymbol{x}}\otimes\hat{\boldsymbol{y}} + \hat{\boldsymbol{y}}\otimes\hat{\boldsymbol{x}})\otimes(\hat{\boldsymbol{x}}\otimes\hat{\boldsymbol{x}} - \hat{\boldsymbol{y}}\otimes\hat{\boldsymbol{y}})\\ &+ 2(\hat{\boldsymbol{y}}\otimes\hat{\boldsymbol{z}} + \hat{\boldsymbol{z}}\otimes\hat{\boldsymbol{y}})\otimes(\hat{\boldsymbol{x}}\otimes\hat{\boldsymbol{z}} + \hat{\boldsymbol{z}}\otimes\hat{\boldsymbol{x}})\\ &- 2(\hat{\boldsymbol{x}}\otimes\hat{\boldsymbol{z}} + \hat{\boldsymbol{z}}\otimes\hat{\boldsymbol{x}})\otimes(\hat{\boldsymbol{y}}\otimes\hat{\boldsymbol{z}} + \hat{\boldsymbol{z}}\otimes\hat{\boldsymbol{y}})],\end{aligned} \tag{6}$$

$$\begin{aligned}\boldsymbol{M}_0^{(4)} = \frac{1}{2\sqrt{70}}[&(\hat{\boldsymbol{x}}\otimes\hat{\boldsymbol{x}} + \hat{\boldsymbol{y}}\otimes\hat{\boldsymbol{y}} - 4\hat{\boldsymbol{z}}\otimes\hat{\boldsymbol{z}})\otimes(\hat{\boldsymbol{x}}\otimes\hat{\boldsymbol{x}} + \hat{\boldsymbol{y}}\otimes\hat{\boldsymbol{y}} - 4\hat{\boldsymbol{z}}\otimes\hat{\boldsymbol{z}})\\ &+ 2\hat{\boldsymbol{x}}\otimes\hat{\boldsymbol{x}}\otimes\hat{\boldsymbol{x}}\otimes\hat{\boldsymbol{x}} + 2\hat{\boldsymbol{y}}\otimes\hat{\boldsymbol{y}}\otimes\hat{\boldsymbol{y}}\otimes\hat{\boldsymbol{y}} - 8\hat{\boldsymbol{z}}\otimes\hat{\boldsymbol{z}}\otimes\hat{\boldsymbol{z}}\otimes\hat{\boldsymbol{z}}\\ &+ (\hat{\boldsymbol{x}}\otimes\hat{\boldsymbol{y}} + \hat{\boldsymbol{y}}\otimes\hat{\boldsymbol{x}})\otimes(\hat{\boldsymbol{x}}\otimes\hat{\boldsymbol{y}} + \hat{\boldsymbol{y}}\otimes\hat{\boldsymbol{x}})\\ &- 4(\hat{\boldsymbol{x}}\otimes\hat{\boldsymbol{z}} + \hat{\boldsymbol{z}}\otimes\hat{\boldsymbol{x}})\otimes(\hat{\boldsymbol{x}}\otimes\hat{\boldsymbol{z}} + \hat{\boldsymbol{z}}\otimes\hat{\boldsymbol{x}})\\ &- 4(\hat{\boldsymbol{y}}\otimes\hat{\boldsymbol{z}} + \hat{\boldsymbol{z}}\otimes\hat{\boldsymbol{y}})\otimes(\hat{\boldsymbol{y}}\otimes\hat{\boldsymbol{z}} + \hat{\boldsymbol{z}}\otimes\hat{\boldsymbol{y}})]\end{aligned} \tag{7}$$

and where $\hat{\boldsymbol{x}}$, $\hat{\boldsymbol{y}}$ and $\hat{\boldsymbol{z}}$ are the unit vectors along a cartesian coordinate system. Note that $G^{(L)}$ modes of $L = 1, 3$ are purely chiral that disappear for racemic mixtures. Using orthonormality properties of the basis $\boldsymbol{M}_0^{(L)}(\boldsymbol{r} - \boldsymbol{r}'/|\boldsymbol{r} - \boldsymbol{r}'|)$ [3], the decomposition (2) allows finally to identify the $G^{(L)}(|\boldsymbol{r} - \boldsymbol{r}'|)$ profiles as:

$$G^{(L)}(|\boldsymbol{r} - \boldsymbol{r}'|) = \boldsymbol{G}(\boldsymbol{r} - \boldsymbol{r}') \cdot \left[\boldsymbol{M}_0^{(L)}\left(\frac{\boldsymbol{r} - \boldsymbol{r}'}{|\boldsymbol{r} - \boldsymbol{r}'|}\right)\right]^*. \tag{8}$$

In the next sections these are calculated for the model system [1,2].

The decomposition (2) is complete in the case of an isotropic chiral liquid. For more complicated structures the set (8) must be supplemented

Downloaded by [University of California, San Diego] at 09:07 22 August 2012

by additional 10 (biaxial) profiles. These will be characterized for cholesteric and blue phases in our forthcoming publication.

III. MODEL

Constant pressure MC simulations are performed for the model chiral liquid crystal introduced by Memmer [1,2]. It defines total intermolecular interaction energy $U(\Omega_i, \Omega_j, \boldsymbol{r}_{ij})$ between the two chiral uniaxial molecules i and j with orientations given by the unit vectors Ω_i, Ω_j and separated by the intermolecular vector $\boldsymbol{r}_{ij}$ as a sum of non-chiral and purely chiral parts. They read

$$U(\Omega_i, \Omega_j, \boldsymbol{r}_{ij}) = U_a(\Omega_i, \Omega_j, \boldsymbol{r}_{ij}) + cU_c(\Omega_i, \Omega_j, \boldsymbol{r}_{ij}), \tag{9}$$

with c being a measure of chirality. $U_a(\Omega_i, \Omega_j, \boldsymbol{r}_{ij})$ represents energy of the non-chiral interaction taken to be of the Gay-Berne form

$$U_a(\Omega_i, \Omega_j, \boldsymbol{r}_{ij}) = 4\varepsilon(\Omega_i, \Omega_j, \boldsymbol{r}_{ij})(R^{-12} - R^{-6}). \tag{10}$$

The effective chiral interaction energy $U_c(\Omega_i, \Omega_j, \boldsymbol{r}_{ij})$ is taken consistent with the chiral dispersion model (see e.g. [6] and references therein) that predicts R^{-7} dependence at separations greater than molecular dimensions. It reads

$$U_c(\Omega_i, \Omega_j, \boldsymbol{r}_{ij}) = -4\varepsilon(\Omega_i, \Omega_j, \boldsymbol{r}_{ij})R^{-7}[(\Omega_i \times \Omega_j) \cdot \boldsymbol{r}_{ij}](\Omega_i \cdot \Omega_j), \tag{11}$$

where $R = (r_{ij} - \sigma(\Omega_i, \Omega_j, \hat{\boldsymbol{r}}_{ij}) + \sigma_0)/\sigma_0$ and $r_{ij} = |\boldsymbol{r}_{ij}|, \hat{\boldsymbol{r}}_{ij} = \boldsymbol{r}_{ij}/r_{ij}$. From the start all quantities in this paper are expressed in dimensionless (reduced) units [1] and notation is simplified by omitting the superscript *, usually introduced to indicate dimensionless quantities. For the Gay-Berne part we used a parameterization suitable for calamitic molecules [7]: $\sigma_e/\sigma_s = 3$, $\epsilon_e/\epsilon_s = 0.2, \mu = 1$ and $\nu = 2$.

We should mention that the effective interaction Eq. (9), although accounting for experimentally observed chiral phases, their sequence and symmetry, seems to have only a qualitative importance for chiral systems. A reason for that are molecular-level values for the cholesteric pitch and for the lattice spacing of the cubic blue phases that follow from the simulations. We do not know as whether more 'realistic' (smaller) values of the chirality parameter c Eq. (9), would yield predictions closer to experimental ones. It would require time-consuming simulations on very large systems, which are not possible at present. However, the observation of the *stable* cholesteric- and blue phases with the molecular-level parameters is certainly very interesting and provides sufficient motivation for more detailed studies presented here.

Downloaded by [University of California, San Diego] at 09:07 22 August 2012

Downloaded by [University of California, San Diego] at 09:07 22 August 2012

In order to overcome at least part of the difficulties mentioned in [1] we carried out the MC simulations in NPT ensemble for a system of moderate size (1000 particles). As usual a trial configuration was generated by a random translation and rotation of an arbitrarily chosen molecule, followed by a random change of randomly chosen box edge. Starting point configuration consisted of molecules placed and oriented in a way characteristic for isotropic phase. Simulations were performed in the temperature-chirality plane with focus on the region where, according to [1,2], cubic blue phases and isotropic phases were present and where the phase known as BPIII was suspected to stabilize ($c \approx 2.0$).

For chiralities c = 0.8, 1.2, 1.6, 2.2 system was equilibrated in a range of temperatures where it exhibited cubic and completely disordered liquid phases. For each chirality we started simulation from lower temperatures and we increased it until structure has disappeared. Number of cycles taken for equilibration was varying between 100000–500000 and production run consisted of 100000 additional cycles. After every 10 cycles of the production run a complete configuration was saved and served as a member of ensemble used for computing of the two-point correlation function and of the excess specific heat in a subsequent step.

IV. RESULTS

The two modes, denoted $G^{(1)}$ and $G^{(3)}$, vanish for racemic mixtures. Hence, they provide a prime characteristic of chiral liquid crystals. Exemplary profiles of $G^{(1)}$ and $G^{(3)}$ are given in Figures (1, 2) for four different chiralities and for various temperatures. The complementary $G^{(0)}$, $G^{(2)}$ and $G^{(4)}$ modes are also given for comparison

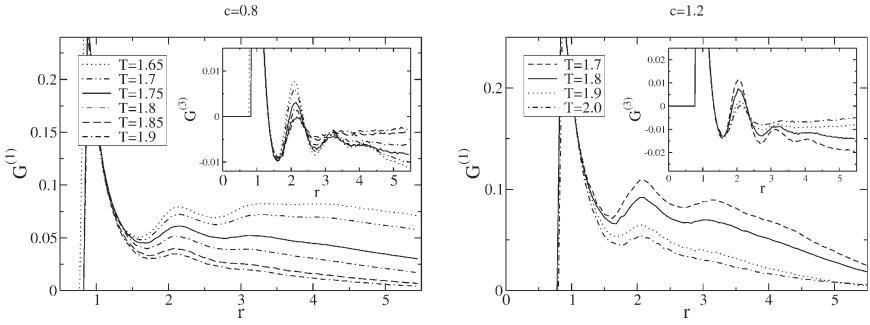

FIGURE 1 Left, $G^{(1)}$ with $G^{(3)}$ as inset for $c = 0.8$; right, $G^{(1)}$ with $G^{(3)}$ as inset for $c = 1.2$.

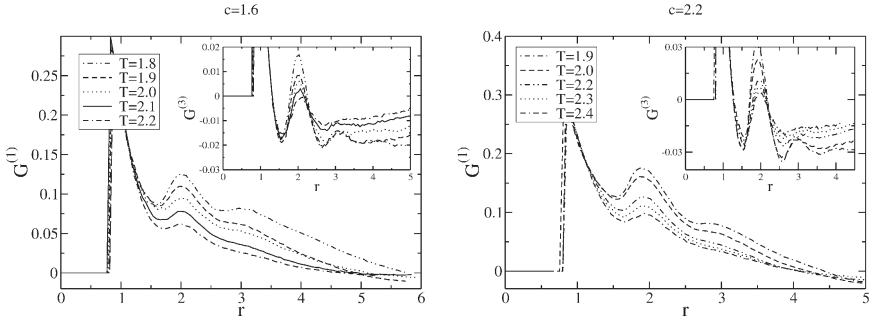

FIGURE 2 Left, $G^{(1)}$ with $G^{(3)}$ as inset for $c = 1.6$; right, $G^{(1)}$ with $G^{(3)}$ as inset for $c = 2.2$.

(see Figs. (3–5)). Both the leading gap for $r < 1$ and the strongest peaks correspond to the system scale given by a single molecule size. Nonzero values of the profiles at large distances indicate on long-range molecular order of BPI or BPII type. As expected correlations are getting smaller with increasing temperature. Also a short-range order is present in the isotropic phase, as expected.

For chirality parameter $c = 0.8$ our results, Figure (l), are consistent with those of Memmer [1]. At temperature $T = 1.65$ we observe a stable phase, which from the analysis of snapshots is classified as BPII. With increasing temperature it transforms directly to the isotropic liquid at $T \approx 1.75$ (see the excess specific heat data in Fig. (6)). No further phase transition to second isotropic liquid was detected with increasing temperature and with assumed temperature scan, which means that BPIII is not stable at $c = 0.8$.

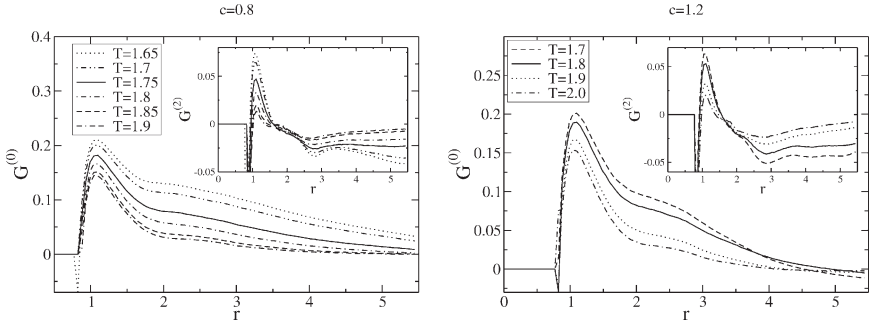

FIGURE 3 Left, $G^{(0)}$ with $G^{(2)}$ as inset for $c = 0.8$; right,$G^{(0)}$ with $G^{(2)}$ as inset for $c = 1.2$.

Downloaded by [University of California, San Diego] at 09:07 22 August 2012

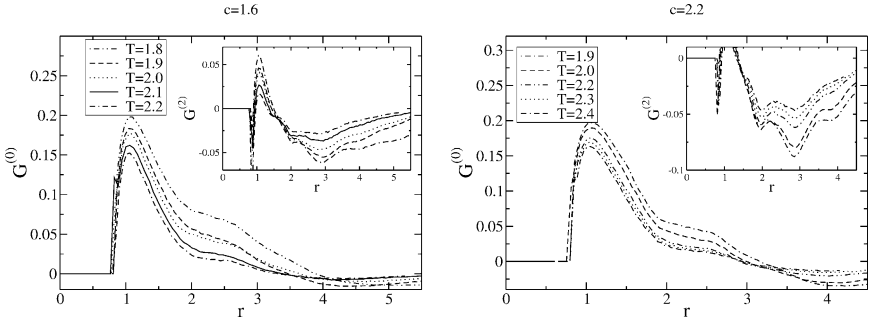

FIGURE 4 Left, $G^{(0)}$ with $G^{(2)}$ as inset for $c = 1.6$; right, $G^{(0)}$ with $G^{(2)}$ as inset for $c = 2.2$.

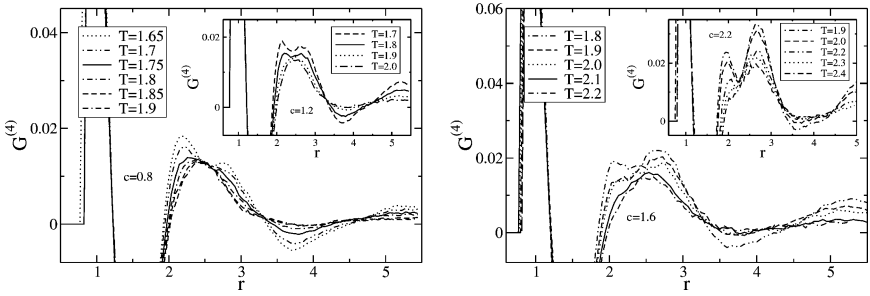

FIGURE 5 Left, $G^{(4)}$ for $c = 0.8$ and for $c = 1.2$ (inset); right, $G^{(4)}$ for $c = 1.6$ and for $c = 2.2$.

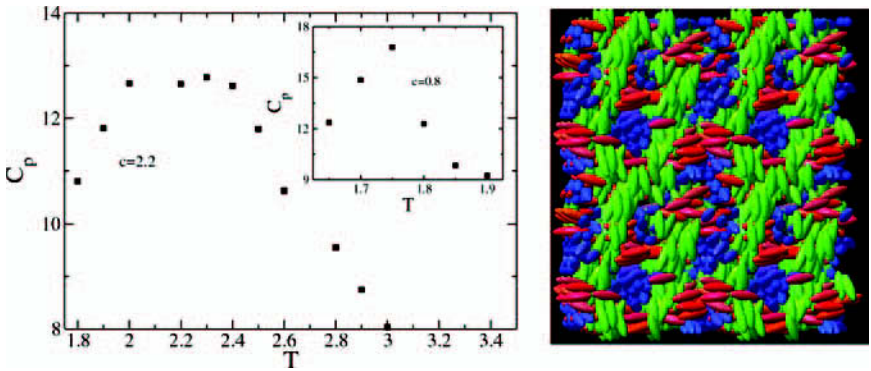

FIGURE 6 Left, excess heat capacity for $c = 2.2$ and $c = 0.8$ (inset); right, snapshot of molecular configuration for temperature $T = 1.9$ and chirality $c = 2.2$. For clarity only those particles are visible whose main axes are aligned along box edges.

Downloaded by [University of California, San Diego] at 09:07 22 August 2012

At chiralities c = 1.2, 1.6 the ordered phase observed at low temperatures (T = 1.7, 1.8) is classified as BPI. The shape of the correlations (see the diagrams in Figs. (1–5)) are different from what we obtained for c = 0.8. Also it is found that the character of the third peak of the correlations changes as temperature and chirality change (see e.g., maximum of $G^{(1)}(r)$ at $r \approx 3$ (Figs. (1,2))). This may indicate on structure evolution from BPI to BPIII (or BPII). As the specific heat data show a broad maximum, which partly splits into two peaks at $c = 2.2$ Figure (6), and correlation profiles drop to zero very fast for $c = 2.2$ (see Figs. (2, 4)), the first option seems more likely (see Fig. (6) for exemplary snapshot). However for the system size considered more quantitative predictions are not possible, in particular a question of the critical point cannot be resolved. In order to make simulations more predictive system size of more than 10000 molecules seems necessary.

REFERENCES

[1] Memmer, R. J. (2001). *Chem. Phys.*, *114*, 8210.
[2] Memmer, R. (2000). *Liq. Cryst.*, *27*, 533.
[3] Longa, L., Cieśla, M., & Trebin, H. R. (2003). *Phys. Rev. E*, *61*, 061705.
[4] Englert, J., Longa, L., Stark, H., & Trebin, H. R. (1998). *Phys. Rev. Let.*, *81*, 1457; Englert, J., Stark, H., Longa, L., & Trebin, H.-R. (2000). *Phys. Rev. E*, *61*, 2759.
[5] Cieśla, M. & Longa, L. (2004). *Phys. Rev. E*, *70*, 012701.
[6] Issaenko, S. A., Harris, A. B., & Lubensky, T. C. (1999). *Phys. Rev. E*, *60*, 578.
[7] Luckhurst, G. R., Stephens, R. A., & Phippen, R. W. (1990). *Liq. Cryst.*, *8*, 451.

Downloaded by [University of California, San Diego] at 09:07 22 August 2012